J Radioanal Nucl Chem (2017) 314:377–386
DOI 10.1007/s10967-017-5414-8

Effect of various environmental factors on the adsorption of U(VI) onto biochar derived from rice straw

Lijia Dong[1] · Jianxia Yang[2] · Yinyan Mou[1] · Guodong Sheng[3] · Linxia Wang[3] · Wensheng Linghu[3] · Abdullah M. Asiri[4] · Khalid A. Alamry[4]

Received: 31 May 2017 / Published online: 22 August 2017

Abstract Herein, we used biochar pyrolyzed from rice straw to adsorb uranium (U) from aqueous solutions. The adsorption of U(VI) on biochar was strongly dependent on pH but independent on ionic strength. HA/FA enhanced the sorption at pH <6.8 while inhibited the sorption at pH >6.8. The sorption reached equilibrium within 3 h, which was not mediated by pH. The adsorption process was spontaneous and endothermic, and enhanced at higher temperature. However, the influence of temperature was negligible at low initial U(VI) concentrations. Therefore, biochar derived from rice straw may be a promising adsorbent for the removal of U(VI).

Keywords Uranium · Biochar · Sorption · Ionic strength · Humic acid · Thermodynamic data

✉ Wensheng Linghu
wslinghu@usx.edu.cn

[1] School of Life Sciences, Shaoxing University, Huancheng West Road 508, Shaoxing 312000, Zhejiang, People's Republic of China

[2] State Key Laboratory of Vegetation and Environmental Change, Institute of Botany, Chinese Academy of Sciences, Beijing 100093, China

[3] School of Chemistry and Chemical Engineering, Shaoxing University, Huancheng West Road 508, Shaoxing 312000, Zhejiang, People's Republic of China

[4] Chemistry Department, Faculty of Science, King Abdulaziz University, Jeddah 21589, Saudi Arabia

Introduction

Uranium (U) is the predominant fuel of nuclear energy used in nuclear industry, which has been regarded as a potential alternative to fossil fuels according to its economical and clean characteristics [1–6]. However, U, existing primarily as the UO_2^{2+} ions in aqueous solutions, starts as a source and ends up as a final waste component in nuclear fuel cycle [1–3]. Once the disposed U is discharged into environment, it will be very harmful to the soils, surface water, and groundwater. Eventually it will inevitably accumulate in the body of human beings through food chains [7]. Due to long half-life, natural radioactivity, extreme chemical toxicity, and strong complexation affinity for organic ligands, excess exposure to U can cause serious diseases, even death [2, 7]. In consideration of this toxic characteristic, it is vital to seek methods for U(VI) removal or remediation from wastewater and groundwater [2–7].

Until recently, dozens of treatment methods such as extraction [8], ion-exchange [9], chemical precipitation [10], membrane dialysis [11], adsorption [12–14], have been employed to preconcentrate and separate uranium component. Among the methods, sorption technique is widely used for the remediation of contaminated environment on account of its high efficiency, low cost, environmental friendliness, and large-scale practicability [15]. A great number of adsorbents, such as bentonite [16], activated carbon [17], graphene oxides [18], bio-nanocomposites [19], carbonaceous nanofibers [3], zerovalent iron nanoparticles [5], titanate nanotubes [6], amine-functionalized MCM-41 [20], Fe_3O_4@Gelatin [21], were proved to be capable in the decontamination of U(VI)-bearing effluents.

Biochar synthesized through pyrolysis of plant-based biomass is a stable carbon-rich adsorbent. In contrast with

activated carbon, biochar pyrolyzed at relatively low temperature (<700 °C) has been found owning more functional groups and mineral ash [22], which endows biochar with a potential sorbent for lots of hazardous cations/anions [23–25]. For example, dairy-manure biochar removed nearly 100% Pb with the initial concentration of 100 mg L^{-1} [23]. Similarly, by using biochar derived from invasive water hyacinth, nearly 100% Cd with the initial concentration equal to or less than 50 mg L^{-1} was removed from aqueous solution [25]. These results implied a promising application of biochar in removal of toxic and even radioactive metal elements from aqueous solution.

In this study, we converted rice straw into biochar to investigate its practical application in the adsorption of U(VI) in aqueous solution. Therefore, the objectives of this work were: (1) to characterize biochar to clarify its surface properties; (2) to investigate the adsorption of U(VI) on biochar; (3) to study the effect of pH, ionic strength, humic acid (HA)/fulvic acid (FA), contact time, temperature, and initial concentration on U(VI) adsorption; (4) to calculate the thermodynamic data from the temperature-dependent sorption isotherms.

Experimental

Materials

The rice straw was collected from Shaoxing city in Zhejiang province, China. The dried plants were crushed and ground to <1.0 mm particle size. Then the ground particles were pyrolyzed at 700 °C in a pyrolyzer under no supply of air. Slow pyrolysis was conducted at a rate of 7 °C min^{-1} and a holding time of 2 h was set for complete carbonization.

U(VI) stock solution was prepared by dissolving $UO_2(NO_3)_2{\cdot}6H_2O$ into double distilled water purged by N_2 gas and then diluted to the required concentration. All chemicals were commercially purchased as analytical reagents and used without further purification.

HA and FA were extracted from the soil in Hua-Jia county (Gansu province, China), and their physicochemical properties had been studied in detail previously [4, 26–28].

Characterization of biochar

The SEM and TEM images were obtained using a field emission scanning electron microscope (JSM-6360LV, Japan) and a transmission electron microscope (JEM-1011, Japan) instrument, respectively. The FT-IR spectra of the biochar was recorded with a FT-IR spectrometer (NEXUS, America) in the range of wavelength 4000–400 cm^{-1} to characterize its surface functional groups. The spectral resolution was set to 2 cm^{-1} and the range of energy ratio was 25–40%.

Batch adsorption experiments

Batch adsorption experiments of U(VI) on biochar derived from rice straw were conducted in polyethylene tubes under N_2 conditions at three different temperatures, i.e., 293, 313 and 333 K. Briefly, the stock suspensions of biochar, $NaClO_4$, HA/FA, UO_2^{2+} solution, and Milli-Q water were added in above-mentioned tubes to achieve the desired concentrations of different components. The ratio of the biochar amount to the solution volume was 0.66 g L^{-1}. The pH values of the adsorption systems were adjusted with negligible volumes of 0.1 or 0.01 mol L^{-1} HNO_3 and/or NaOH solutions. Herein, the deviation for the ratio of the amount of U(VI) to the solution volume is less than 1% duo to the pH adjustment. To ensure adsorption equilibrium, the mixed solutions were gently shaken for 24 h. Then the samples were subjected to separated solid and liquid phases through centrifugation at 9000 rpm for 30 min.

The U(VI) concentration in the supernatant was analyzed by spectrophotometry at 681 nm. The U(VI) removal percent from aqueous solution (U(VI) removal $\% = (C_0 - C_e)/C_0 \times 100\%$) and sorption amount onto biochar ($q_e = (C_0 - C_e) \times V/m$) were calculated from the initial U(VI) concentration (C_0, mol L^{-1}), the final U(VI) concentration (C_e, mol L^{-1}), the biochar mass (m, g), and the suspension volume (V, L).

All batch experiments were conducted in duplicates and each data point was measured in triplicates in order to ensure the experimental repeatability and improve data accuracy. The relative errors of the experimental data were less than 5%.

Results and discussion

Characterization

The SEM, TEM, and FT-IR characterization of biochar derived from rice straw are shown in Fig. 1. We can observe from the SEM image (Fig. 1a) that the stratified structure of biochar is formed and randomly accumulated in loose state. Furthermore, both of the surface and edge of biochar are rough. This structure may provide more space for the contact between metal ions and biochar. The TEM image (Fig. 1b) indicates that the aggregation of biochar particles is heterogeneous and loose in aqueous solutions, which increases the surface area of biochar. In other words, the stratified structure of biochar and loose distribution of biochar particles may endow the biochar derived from rice

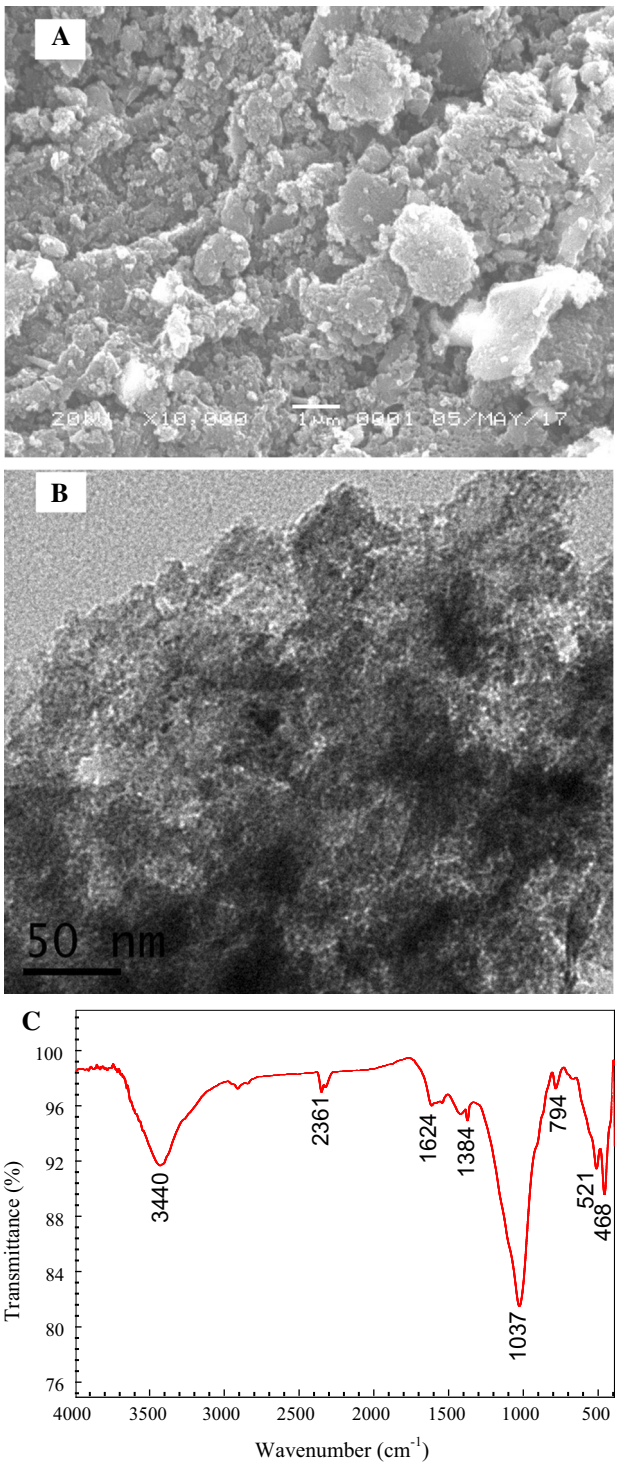

Fig. 1 SEM (**a**), TEM (**b**), and FT-IR spectrum (**c**) of biochar derived from rice straw

straw with excellent adsorptive ability. The FT-IR spectrum shows functional groups on biochar (Fig. 1c). The band at 3440 cm^{-1} is assigned to O–H stretching vibration of biochar [29–31]. The band at 2361 cm^{-1} is assigned to C≡C and –C≡N triple bonds or accumulates in C=C=C– and –N=C=O double bonds [31, 32]. In the middle wavenumber range, FT-IR spectra of biochar shows aromatic C=C (1624 cm^{-1}), carboxyl O=C–O (1384 cm^{-1}), and alkoxy C–O (1037 cm^{-1}) stretching vibrations, respectively [18]. In the low wavenumber range, the bands at 794, 521, and 468 may be assigned to the integrated crystalline structure of biochar [33].

Effect of contact time

Figure 2 shows that the sorption kinetics of U(VI) on biochar under 0.01 mol L^{-1} $NaClO_4$ and three pH values conditions, i.e., pH 4.48, 5.26, 6.15. The percentage of U(VI) removal rapidly increases in the first 1 h, and then slowly increases until the sorption process achieves equilibrium after 3 h (Fig. 2a). This tendency is similar under three pH values conditions, i.e., each U(VI) removal in each pH condition reaches high-level within 3 h (Fig. 2a). The initial fast removal rate can be attributed to a large

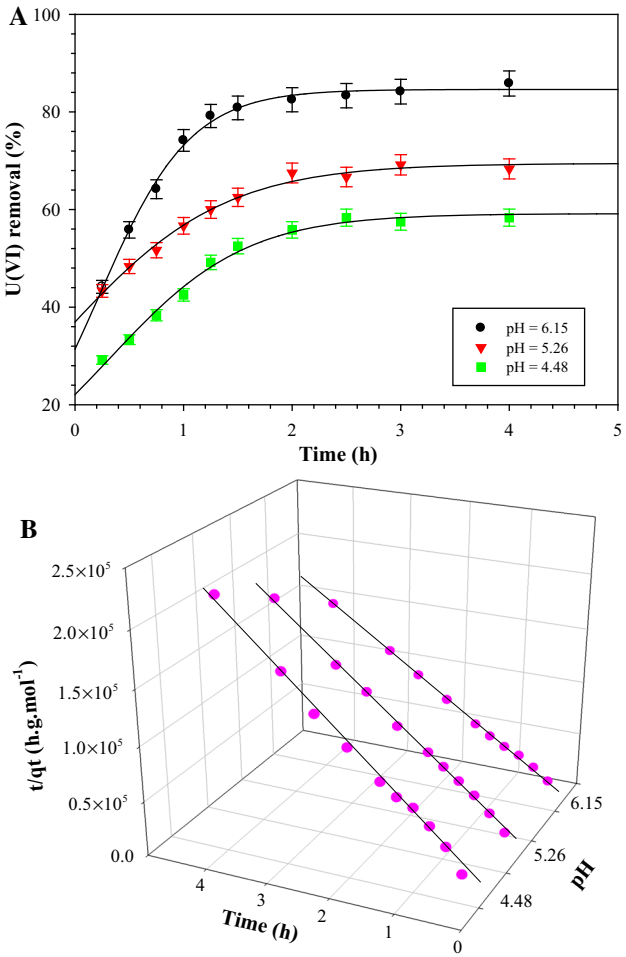

Fig. 2 Effect of contact time on U(VI) removal percentage (**a**) and U(VI) sorption (**b**) onto biochar with different pH values. I ($NaClO_4$) = 0.01 mol L^{-1}, T = 293 K, $C_{U(VI)initial}$ = 2 × 10^{-5} mol L^{-1}, m/V = 0.66 g L^{-1}

number of adsorption sites available, which implies that the sorption is dominated by chemical adsorption or surface complexation rather than physical adsorption [21, 34, 35]. With the gradual occupancy of these sites, the sorption efficiency becomes less efficient. Therefore, in the following experiments, we selected a contact time of 24 h to ensure complete adsorption equilibrium.

The above results suggest that the contact time of U(VI) adsorption on biochar may not mediated by the pH value. However, it is observed that the removal percent evidently increases with an increase of pH values (Fig. 2d). Therefore, we can conclude that the binding time of U(VI) with the surface sites of biochar is slightly affected by pH values of solutions, although the quantity of binding was strongly affected by pH values.

The sorption rate is mainly dependent on the surface characteristics and diffusion resistance of sorbents. Therefore, appropriate kinetic models, either pseudo-first order or pseudo-second order models, generally provide useful information for determining the underlying uptake mechanisms [18, 21]. In view of this, both pseudo-first and -second order models were applied to the kinetic data of U(VI) on biochar. Finally, the pseudo-second order kinetic was found to better describe the sorption process, which is calculated by the following expression [36, 37]:

$$\frac{t}{q_t} = \frac{1}{2kq_e^2} + \frac{t}{q_e} \quad (1)$$

where q_e and q_t refer to the uptake capacity of U(VI) (mol g^{-1}) at equilibrium time and time t (h), respectively; k (g (mol h)$^{-1}$) is the rate constant. The three-dimensional linear plot of t/qt versus t under three pH values conditions is shown in Fig. 2b. The corresponding vales of k and q_e are shown in Table 1. From this table, we can see that the correlation coefficient for each line is up to 0.999, which suggests that the kinetic uptake process in three pH values can be well described by the pseudo-second-order model. Once again, this phenomenon indicates that the sorption process is chemical but not physical sorption [37].

Table 1 Kinetic parameters of U(VI) adsorption on biochar derived from rice straw with three different pH values (4.48, 5.26, and 6.15). I ($NaClO_4$) = 0.01 mol L^{-1}, T = 293 K, $C_{U(VI)initial} = 2 \times 10^{-5}$ mol L^{-1}, m/V = 0.66 g L^{-1}

pH values	Pseudo-second-order parameters			
	q_e (mol g^{-1})	K (g mol^{-1} h^{-1})	r^2	P value
4.48	2.799×10^{-5}	2.160	0.999	<0.001
5.26	3.008×10^{-5}	2.829	0.999	<0.001
6.15	3.375×10^{-5}	2.441	0.999	<0.001

Effect of pH and ionic strength

Figure 3 shows the effect of pH on the adsorption of U(VI) onto biochar in three different electrolyte concentrations (i.e., I ($NaClO_4$) = 0.1, 0.01, 0.001 mol L^{-1}). It is clear that pH significantly influences the sorption behavior of U(VI). Specifically, the removal percentage of U(VI) significantly increases from 31.67 to 99.17% with increasing pH values from 3.0 to 6.8, whereas the high-level adsorption and decreased adsorption are observed in the pH range of 7.3–9.2. Similar results were observed for U(VI) sorption to carbonaceous nanofibers [3], titanate nanotubes [6], MCM-41-NH_2 [20], Fe_3O_4@Gelatin [21], SiO_2 [38], etc. The reasons for the increasing sorption can be attributed to a decrease in the competition between protons (H^+) and U(VI) for surface sites of biochar with an increase in pH values [27, 39–41]. Because UO_2^{2+} or $(UO_2)_3(OH)_5^+$ and $(UO_2)_4(OH)_7^+$ are the dominant species at low pH (pH <8.0), while both H^+ and these positive U(VI) ions can generate electrostatic repulsion on biochar surface [3, 4, 42]. The adsorption and subsequent precipitation process, such as the formation of schoepite, may result in the high-level removal of U(VI) on biochar at pH 6.8 [3]. The dramatic decrease in U(VI) adsorption at pH >7.3 may be due to the occurrence of dissolved inorganic carbon or the formation of negative U(VI) ions at high pH values, such as $(UO_2)_3(OH)_7^-$, $UO_2(CO_3)_2^{2-}$, $UO_2(CO_3)_3^{4-}$. These ions are difficult to be retained on the negatively charged surfaces of sorbents because of electrostatic repulsion [3, 4, 43, 44].

Meanwhile, as shown in Fig. 3, pH effects on the adsorption of U(VI) are similar in each $NaClO_4$ concentration. This result indicates that U(VI) sorption is independent on ionic strength, implying that the sorption of

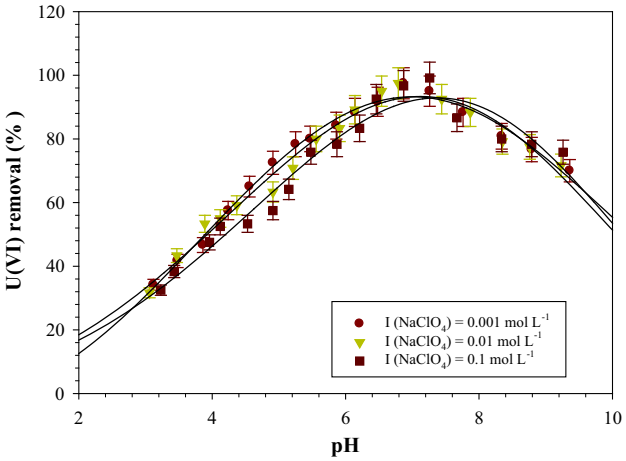

Fig. 3 Percentage removal of U(VI) from solutions with different pH by biochar derived from rice straw at three concentrations of $NaClO_4$. $T = 293$ K, $C_{U(VI)initial} = 2 \times 10^{-5}$ mol L^{-1}, m/V = 0.66 g L^{-1}

U(VI) on biochar derived from rice straw is mainly dominated by inner-sphere surface complexation. Generally speaking, when the adsorption is dependent on pH but not on the ionic strength, the sorption is mainly controlled by inner-sphere surface complexation; the opposite situation indicates that the sorption is mainly controlled by outer-sphere surface complexation or ion exchange [18, 45–47]. In view of these conclusions, we can infer that the adsorption of U(VI) on biochar is predominated by inner-sphere complexation.

Effect of humic substances

Humic substances play an important role in controlling the transformation and migration behaviors of radionuclides and heavy metal ions. Hence, to study the effect of humic substances on adsorption is vital for understanding sorption characteristics of adsorbents. The pH dependence of U(VI) sorption on biochar in the absence and presence of HA/FA is shown in Fig. 4. The presence of HA/FA enhances the uptake of U(VI) at pH <6.8, while inhibits the sorption at pH >6.8. Simultaneously, there is no significant gap between HA and FA addition at the whole pH range. The results are similar to the effect of HA/FA on the sorption of Eu(III) on graphene oxide, and of U(VI) on MX-80 Bentonite [18, 48]. Generally, there is strong interaction between HA/FA and U(VI) due to rich "adsorbed" groups included in HA/FA. And the complexation between HA/FA and U(VI) is stronger than U(VI) and adsorbents. Therefore, the negatively-charged HA/FA can be easily adsorbed on the positively-charged biochar at low pH values. At the same time, the positively-charged U(VI) ions can easily form complexes with FA/HA adsorbed on the surface of biochar, which enhances the sorption of U(VI) on FA/HA-biochar hybrids. At high values, the solubility of FA/HA increases and the biochar becomes negatively-charged, which leads to the electrostatic repulsion. Furthermore, a part of free stable FA/HA–U(VI) complexes are formed in solutions. Thus, the negatively-charged FA/HA is weakly adsorbed on the surface of biochar, leading to the decrease of U(VI) sorption on biochar. As the general regards [34, 49], our results also prove that the presence of HA/FA enhances the adsorption of metal ions at low pH values while inhibits the adsorption of metal ions at high pH values.

Effects of initial concentration and temperature

The percentage of U(VI) removal by biochar at different temperatures and initial concentrations is given in Fig. 5. The amount of U(VI) sorption decreases with increasing initial U(VI) concentration: from around 95 to 50%. The removal percent is more than 90% at low initial concentration and more than 45% at high initial concentration. Moreover, the influence of temperature is negligible at low initial U(VI) concentrations ($C_0 < 1.7 \times 10^{-5}$ mol L^{-1}) while is significant at high initial U(VI) concentrations ($C_0 > 1.7 \times 10^{-5}$ mol L^{-1}). The result indicates that the U(VI) removal percentage may be affected by interactions between initial concentration and temperature. One explanation is that there are enough sorption sites on the surface of biochar at low initial concentration, while higher temperature enhances the sorption through providing more thermal energy when the sites not enough at high initial concentration [50, 51].

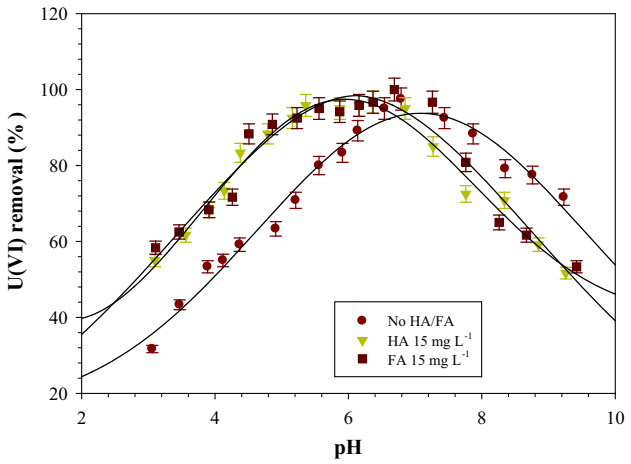

Fig. 4 Percentage removal of U(VI) from solutions with different pH by biochar at three treatments of FA addition, HA addition and no HA/FA addition. I ($NaClO_4$) = 0.01 mol L^{-1}, T = 293 K, $C_{U(VI)initial} = 2 \times 10^{-5}$ mol L^{-1}, m/V = 0.66 g L^{-1}

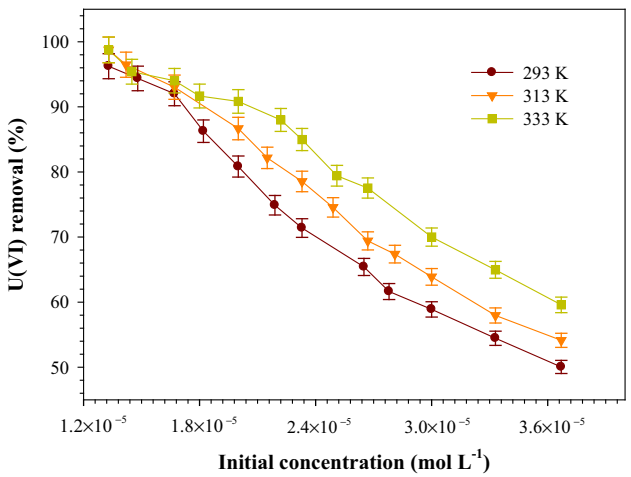

Fig. 5 Percentage removal of U(VI) at different initial concentrations and temperatures. I ($NaClO_4$) = 0.01 mol L^{-1}, m/V = 0.66 g L^{-1}

Adsorption isotherms and thermodynamic study

The adsorption isotherms describe the interactions between adsorbates and adsorbents and provide the most import parameter to design a desired adsorption system [52]. Figure 6 shows that the sorption isotherms of U(VI) on biochar at 293, 313, and 333 K. The amount of U(VI) adsorption in $C_0 > 1.7 \times 10^{-5}$ mol L^{-1} increased with an increase of temperature, suggesting that the sorption is enhanced in higher temperature. To obtain a better understanding on mechanisms of U(VI) adsorption on biochar, four equilibrium models, i.e., Langmuir [53, 54], Freundlich [55], Temkin [56], and Dubinin–Radushkevich (D–R) model [57], were selected to fit the sorption isotherms. Linear form of these isotherm models can be expressed by following equations.

$$\frac{C_e}{q_e} = \frac{1}{K_L q_{max}} + \frac{C_e}{q_{max}} \quad (2)$$

$$\log q_e = \log_F + n \log C_e \quad (3)$$

$$q_e = \frac{RT}{b} \ln A + \frac{RT}{b} \ln C_e \quad (4)$$

$$\ln q_e = \ln q_{max} - \beta \varepsilon^2 \quad (5)$$

where q_{max} (mol g^{-1}) represents the maximum uptake capacity of U(VI) on per weight unit of biochar; K_L (L mol^{-1}) is the Langmuir affinity parameter; K_F (mol^{1-n} L^n g^{-1}) and n are the Freundlich affinity-capacity parameter and exponent, respectively; R is the universal gas constant (8.314 J K^{-1} mol^{-1}), T (K) is the absolute temperature in Kelvin, b is the heat of adsorption, and A is the binding constant; β is the D–R activity constant and ε is the Polanyi potential, which is calculated by RT $\ln(1 + 1/C_e)$; From D–R model, bonding energy of the ion-exchange mechanism (E, KJ g^{-1}) is calculated by $(2\beta)^{-1/2}$.

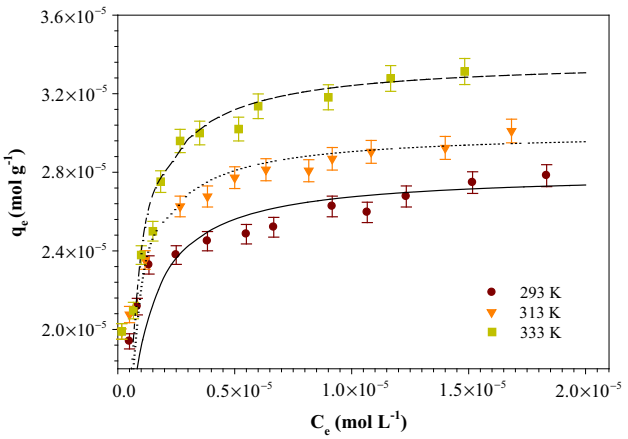

Fig. 6 Sorption isotherms of U(VI) adsorption onto biochar at three different temperatures. I ($NaClO_4$) = 0.01 mol L^{-1}, m/V = 0.66 g L^{-1}

In Fig. 7, linearized Langmuir isotherm, Freundlich isotherm, Temkin isotherm, and D–R isotherm on U(VI) adsorption onto biochar at three temperatures (293, 313 and 333 K) are displayed. The relative parameters calculated from the four isotherm models are listed in Table 2. According to the values of correlation coefficients (r^2), we find that the fitting of Langmuir model is the best among the four models (Table 2). The result suggests that the adsorption process occurs on the functional groups/binding sites on the surface of biochar, and is viewed as homogeneous monolayer coverage. The q_{max} value obtained from Langmuir model increases from 2.799×10^{-5} to 3.375×10^{-5} mol g^{-1} with the temperature increasing from 293 to 333 K (Table 2), which suggests that high temperature is favorable to adsorption. Except for the Langmuir model, the Freundlich, Temkin, and D-R model also fit the data of U(VI) sorption on biochar very well (Table 2; Fig. 7). The n values, gained from the Freundlich model, are less than 1, which indicates that the sorption is favorable under different temperatures. The above results illustrate that the biochar derived from rice straw can be treated as a potential novel adsorbent for the removal of U(VI).

The thermodynamic parameters (ΔH^0, ΔS^0, and ΔG^0) for U(VI) on biochar at three different temperatures can be determined from the temperature dependence, in order to illustrate the thermodynamic properties of adsorption. Gibbs free energy (ΔG^0) is calculated from the relationship:

$$\Delta G^0 = -RT \ln K^0 \quad (6)$$

where K^0 is the equilibrium constant of sorption reaction, and we got the values of $\ln K^0$ by plotting $\ln K^0$ versus C_e and extrapolating C_e to zero [58]. Standard entropy (ΔS^0) and the average standard enthalpy (ΔH^0) are calculated using the following two equations [59], respectively.

$$\left(\frac{\partial \Delta G^0}{\partial \Delta T^0}\right)_p = -\Delta S^0 \quad (7)$$

$$\Delta H^0 = T\Delta S^0 + \Delta G^0 \quad (8)$$

The obtained thermodynamic parameters are listed in Table 3. These parameters provide an insight into understanding the mechanism of the adsorptive interaction of U(VI) with the biochar derived from rice straw. The value of ΔG^0 is negative and become more negative as the temperature increases, suggesting that the adsorption process is spontaneous and more efficient at higher temperature. The possible explanation is that U(VI) is readily desolvated and hence its sorption becomes more favorable at high temperature [18]. The positive value of ΔH^0

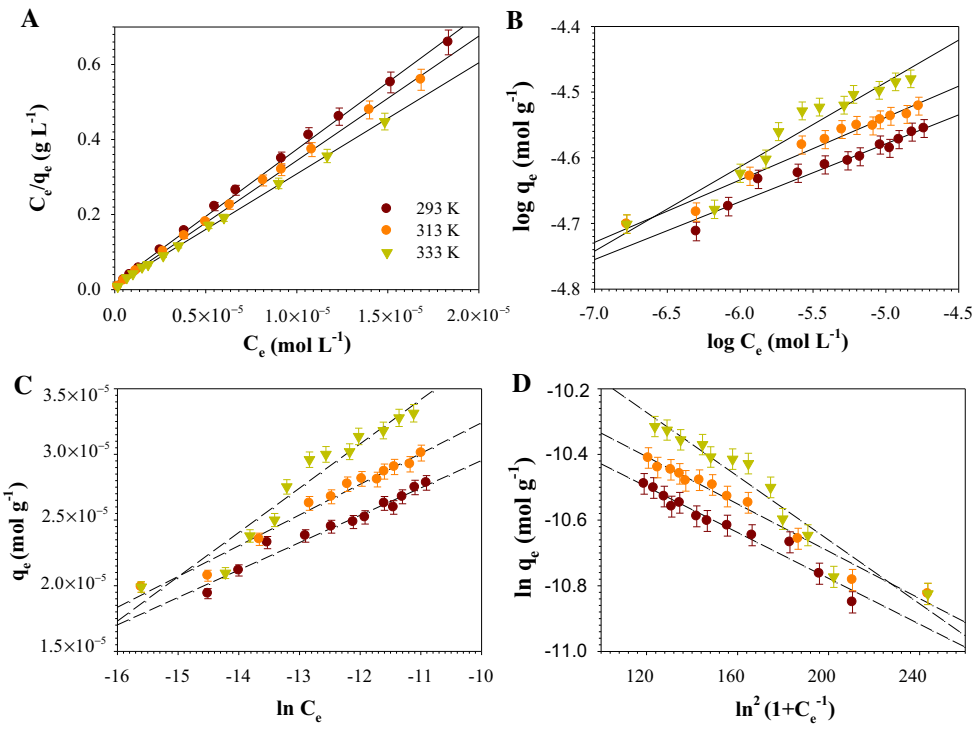

Fig. 7 Linearized Langmuir isotherm (**a**), Freundlich isotherm (**b**), Temkin isotherm (**c**), Dubinin–Radushkevich isotherm (**d**) on U(VI) adsorption for biochar derived from rice straw at 293, 313, and 333 K. I ($NaClO_4$) = 0.01 mol L^{-1}, m/V = 0.66 g L^{-1}

Table 2 Isotherm parameters for U(VI) adsorption onto biochar derived from rice straw at three different temperatures (293, 313 and 333 K). I ($NaClO_4$) = 0.01 mol L^{-1}, $C_{U(VI)initial}$ = 2 × 10^{-5} mol L^{-1}, m/V = 0.66 g L^{-1}

Temperature (K)	q_{max} (mol g^{-1})	K_L (L mol^{-1})	r^2	*P* value
Langmuir model				
293	2.799 × 10^{-5}	2.160	0.999	<0.001
313	3.008 × 10^{-5}	2.829	0.999	<0.001
333	3.375 × 10^{-5}	2.441	0.999	<0.001
	K_F (mol^{1-n} L^n g^{-1})	*n*	r^2	*P* value
Freundlich model				
293	7.281 × 10^{-5}	0.0882	0.954	<0.001
313	8.649 × 10^{-5}	0.0951	0.976	<0.001
333	14.38 × 10^{-5}	0.129	0.931	<0.001
	A	*b*	r^2	*P* value
Temkin model				
293	3.154 × 10^{10}	1.189 × 10^9	0.964	<0.001
313	2.329 × 10^{10}	1.079 × 10^9	0.980	<0.001
333	1.521 × 10^{10}	0.822 × 10^9	0.938	<0.001
	q_{max} (mol g^{-1})	E (KJ g^{-1})	r^2	*P* value
Dubinin-Radushkevich model				
293	4.191 × 10^{-5}	29.148	0.961	<0.001
313	4.655 × 10^{-5}	29.688	0.977	<0.001
333	6.196 × 10^{-5}	28.083	0.932	<0.001

Table 3 Values of thermodynamic parameters for U(VI) adsorption on biochar derived from rice straw at three different temperatures (293 K, 313 K, and 333 K)

T (K)	ΔG^o (KJ mol^{-1})	ΔS^o (J mol^{-1} K^{-1})	ΔH^o (KJ mol^{-1})
293	−23.907	107.118	7.479
313	−25.771		6.686
333	−28.378		4.079

I ($NaClO_4$) = 0.01 mol L^{-1}, $C_{U(VI)initial}$ = 2 × 10^{-5} mol L^{-1}, m/V = 0.66 g L^{-1}

suggests that the adsorption of U(VI) on biochar is an endothermic process, which is an indication of a strong interaction between U(VI) and biochar. One possible reason is that the ions, such as U(VI) solvated in water, are to some extent denuded of their hydration sheath in the process of adsorption, and the dehydration process of ions requires energy. Although the process of ions attaching to the surface of adsorbents is exothermic, the endothermicity of the desolvation process exceeds that of the enthalpy of adsorption to a considerable extent [60, 61]. Therefore, the adsorption process is favored at higher temperature [58, 62]. A positive value of ΔS^0 implies some structure changes in U(VI) and the biochar during the sorption process, leading to an increase in the disorderness at the biochar-solution interface [63, 64]. All the above analyses of thermodynamic parameters indicate that the sorption

process of U(VI) on biochar is spontaneous and endothermic.

Conclusions

In this study, we used biochar derived from rice straw as an adsorbent to remove U(VI) from aqueous solutions. From the results of batch experiments, we could obtain the following conclusions:

(1) Although the sorption amount of U(VI) was strongly affected by pH values, the sorption rate was slightly affected by pH values. The velocities of U(VI) sorption were simulated well by the pseudo-second-order kinetic model, which implied that chemisorption was the rate-controlling mechanism.
(2) The adsorption of U(VI) on biochar was strongly dependent on pH in the range of 3.0–9.2, but independent on ionic strength within the pH range. The result indicated that the sorption of U(VI) on biochar was mainly dominated by inner-sphere surface complexation within the wide pH range.
(3) The adsorption of U(VI) was significantly affected by HA/FA, and this effect was dependent on pH values. The adsorption was enhanced at low pH values, but inhabited at high pH values.
(4) The U(VI) removal percentage could be affected by interactions between initial concentration and temperature: the influence of temperature was negligible at low initial U(VI) concentrations while significant at high initial U(VI) concentrations.
(5) The adsorption isotherms of U(VI) on biochar at three different temperatures could be fitted well by Langmuir, Freundlich, Temkin, and D–R isotherm model, but Langmuir was the best. The sorption of U(VI) on biochar was implied to be homogeneous monolayer coverage and was favorable at higher temperature.
(6) Thermodynamic data indicated that the sorption of process U(VI) on biochar was a spontaneous and endothermic process.
(7) Results of this experiment indicate biochar derived from rice straw could be potentially used as an efficient and promising candidate for the removal of metal ions from aqueous solutions.

Acknowledgements Financial supports from the National Natural Science Foundation of China (21577093), Natural Science Foundation of Zhejiang Province (LY15B070001) is greatly acknowledged.

References

1. Waseem A, Ullah H, Rauf MK, Ahmad I (2015) Distribution of natural uranium in surface and groundwater resources: a review. Crit Rev Environ Sci Technol 45:2391–2423
2. Keith S, Faroon O, Roney N, Scinicariello F, Wilbur S, Ingerman L, Llados F, Plewak D, Wohlers D, Diamond G (2013) Toxicological profile for uranium. Agency for Toxic Substances and Disease Registry (US) 39-175
3. Sun Y, Wu Z, Wang X, Ding C, Cheng W, Yu S, Wang X (2016) Macroscopic and microscopic investigation of U(VI) and Eu(III) adsorption on carbonaceous nanofibers. Environ Sci Technol 50:4459–4467
4. Zhao D, Wang X, Yang S, Guo Z, Sheng G (2012) Impact of water quality parameters on the sorption of U(VI) onto hematite. J Environ Radioact 103:20–29
5. Sheng G, Yang P, Tang Y, Hu Q, Li H, Ren X, Hu B, Wang X, Huang Y (2016) New insights into the primary roles of diatomite in the enhanced sequestration of UO_2^{2+} by zerovalent iron nanoparticles: an advanced approach utilizing XPS and EXAFS. Appl Catal B Environ 193:189–197
6. Sheng G, Hu J, Alsaedi A, Shammakh W, Monaquel S, Ye F, Li H, Huang Y, Alshomrani A, Hayat T, Ahmad B (2015) Interaction of uranium(VI) with titanate nanotubes by macroscopic and spectroscopic investigation. J Mol Liq 212:563–568
7. Brugge D, Buchner V (2011) Health effects of uranium: new research findings. Rev Environ Heal 26:231–249
8. Agrawal YK, Shrivastav P, Menon SK (2000) Solvent extraction, separation of uranium(VI) with crown ether. Sep Purif Technol 20:177–183
9. Rao TP, Metilda P, Gladis JM (2006) Preconcentration techniques for uranium(VI) and thorium(IV) prior to analytical determination-an overview. Talanta 68:1047–1064
10. Mellah A, Chegrouche S, Barkat M (2007) The precipitation of ammonium uranyl carbonate (AUC): thermodynamic and kinetic investigations. Hydrometallurgy 85:163–171
11. Bockris J (2013) Electrochemistry of cleaner environments. Springer Science & Business Media, New York
12. Wang X, Zhu G, Guo F (2013) Removal of uranium(VI) ion from aqueous solution by SBA-15. Ann Nucl Energy 56:151–157
13. Zou Y, Wang X, Khan A, Wang P, Liu Y, Alsaedi A, Hayat T, Wang X (2016) Environmental remediation and application of nanoscale zero-valent iron and its composites for the removal of heavy metal ions: a review. Environ Sci Technol 50:7290–7304
14. Jemison NE, Johnson TM, Shiel AE, Lundstrom CC (2016) Uranium isotopic fractionation induced by U(VI) adsorption onto common aquifer minerals. Environ Sci Technol 50:12232–12240
15. Yang S, Zong P, Hu J, Sheng G, Wang Q, Wang X (2013) Fabrication of β-cyclodextrin conjugated magnetic HNT/iron oxide composite for high-efficient decontamination of U (VI). Chem Eng J 214:376–385
16. Verma PK, Pathak P, Mohapatra M, Yadav AK, Jha S, Bhattacharyya D, Mohapatra PK (2015) Spectroscopic investigations on sorption of uranium onto suspended bentonite: effects of pH, ionic strength and complexing anions. Radio Chim Acta 103:293–303
17. Mellah A, Chegrouche S, Barkat M (2006) The removal of uranium(VI) from aqueous solutions onto activated carbon: kinetic and thermodynamic investigations. J Colloid Interface Sci 296:434–441
18. Hu B, Hu Q, Li X, Pan H, Tang X, Chen C, Huang C (2017) Rapid and highly efficient removal of Eu(III) from aqueous solutions using graphene oxide. J Mol Liq 229:6–14

19. Ding C, Cheng W, Sun Y, Wang X (2015) Novel fungus-Fe_3O_4 bio-nanocomposites as high performance adsorbents for the removal of radionuclides. J Hazard Mater 295:127–137
20. Tang P, Shen J, Hu Z, Bai G, Wang M, Peng B, Shen R, Linghu W (2016) High-efficient scavenging of U(VI) by magnetic Fe_3O_4@gelatin composite. J Mol Liq 221:497–506
21. Xiao J, Jing Y, Yao Y, Xie S, Wang X, Shi C, Jia Y (2016) Synthesis of amine-functionalized MCM-41 and its highly efficient sorption of U(VI). J Radioanal Nucl Chem 310:1001–1011
22. Kloss S, Zehetner F, Dellantonio A, Hamid R, Ottner F, Liedtke V, Schwanninger M, Gerzabek MH, Soja G (2012) Characterization of slow pyrolysis biochars: effects of feedstocks and pyrolysis temperature on biochar properties. J Environ Qual 41:990–1000
23. Cao X, Harris W (2010) Properties of dairy-manure-derived biochar pertinent to its potential use in remediation. Bioresource Technol 101:5222–5228
24. Ahmad M, Rajapaksha AU, Lim JE, Zhang M, Bolan N, Mohan D, Vithanage D, Lee SS, Ok YS (2014) Biochar as a sorbent for contaminant management in soil and water: a review. Chemosphere 99:19–33
25. Zhang F, Wang X, Yin D, Peng B, Tan C, Liu Y, Tan X, Wu S (2015) Efficiency and mechanisms of Cd removal from aqueous solution by biochar derived from water hyacinth (*Eichhornia crassipes*). J Environ Manag 153:68–73
26. Sheng G, Wang S, Hu J, Lu Y, Li J, Dong Y, Wang X (2009) Adsorption of Pb(II) on diatomite as affected via aqueous solution chemistry and temperature. Colloids Surf A 339:159–166
27. Tan X, Wang X, Geckeis H, Rabung T (2008) Sorption of Eu(III) on humic acid or fulvic acid bound to alumina studied by SEM-EDS, XPS, TRLFS and batch techniques. Environ Sci Technol 42:6532–6537
28. Sheng G, Li J, Shao D, Hu J, Chen C, Chen Y, Wang X (2010) Adsorption of copper(II) on multiwalled carbon nanotubes in the absence and presence of humic or fulvic acids. J Hazard Mater 178:333–340
29. Kim WK, Shim T, Kim YS, Hyun S, Ryu C, Park YK, Jung J (2013) Characterization of cadmium removal from aqueous solution by biochar produced from a giant *Miscanthus* at different pyrolytic temperatures. Bioresource Technol 138:266–270
30. Tong XJ, Li JY, Yuan JH, Xu RK (2011) Adsorption of Cu(II) by biochars generated from three crop straws. Chem Eng J 172:828–834
31. Kołodyńska D, Krukowska J, Thomas P (2017) Comparison of sorption and desorption studies of heavy metal ions from biochar and commercial active carbon. Chem Eng J 307:353–363
32. Samsuri AW, Sadegh-Zadeh F, Seh-Bardan BJ (2013) Adsorption of As(III) and As(V) by Fe coated biochars and biochars produced from empty fruit bunch and rice husk. J Environ Chem Eng 1:981–988
33. Zong P, Wang H, Pan H, Zhao Y, He C (2013) Application of NKF-6 zeolite for the removal of U(VI) from aqueous solution. J Radioanal Nucl Chem 295:1969–1979
34. Wang XX, Yang SB, Shi WQ, Li JX, Wang XK, Hayat T (2015) Different interaction mechanisms of Eu(III) and ^{243}Am(III) with carbon nanotubes studied by batch, spectroscopy technique and theoretical calculation. Environ Sci Technol 49:11721–11728
35. Wang X, Lu S, Chen L, Li J, Dai S, Wang X (2015) Efficient removal of Eu(III) from aqueous solutions using super-adsorbent of bentonite-polyacrylamide composites. J Radioanal Nucl Chem 306:497–505
36. Ho Y (2006) Review of second-order models for adsorption systems. J Hazard Mater 37:681–689
37. Ho Y, McKay G (1999) Pseudo-second order model for sorption processes. Process Biochem 34:451–465
38. Comarmond MJ, Steudtner R, Stockmann M, Heim K, Müller K, Brendler V, Payne TE, Foerstendorf H (2016) The sorption process of U(VI) onto SiO_2 in the presence of phosphate: from binary surface species to precipitation. Environ Sci Technol 50:11610–11618
39. Fairhurst AJ, Warwick P, Richardson S (1995) The influence of humic acid on the adsorption of europium onto inorganic colloids as a function of pH. Colloids Surf A 99:187–199
40. Fairhurst AJ, Warwick P (1998) The influence of humic acid on europium-mineral interactions. Colloids Surf A 145:229–234
41. Janot N, Benedetti MF, Reiller PE (2013) Influence of solution parameters on europium (III), -Al_2O_3, and humic acid interactions: macroscopic and time-resolved laser-induced luminescene data. Geochim Cosmochim Acta 123:35–54
42. Sun YB, Zhang R, Ding CC, Wang XX, Cheng WC, Chen CL, Wang XK (2016) Adsorption of U(VI) on sericite in the presence of Bacillus subtilis: a combined batch, EXAFS and modeling techniques. Geochim Cosmochim Acta 180:51–65
43. Waite TD, Davis JA, Payne TE, Waychunas GA, Xu N (1994) Uranium(VI) adsorption to ferrihydrite: application of a surface complexation model. Geochim Cosmochim Acta 58:5465–5478
44. Sheng G, Shao X, Li Y, Li J, Dong H, Cheng W, Gao X, Huang Y (2014) Enhanced removal of U(VI) by nanoscale zerovalent iron supported on Na-bentonite and an investigation of mechanism. J Phys Chem A 118:2952–2958
45. Hayes KF, Leclie JO (1987) Modeling ionic strength effect on cation adsorption at hydrous oxide/solution interfaces. J Colloid Interface Sci 115:564–572
46. Sun YB, Yang SB, Chen Y, Ding CC, Cheng WC, Wang XK (2015) Adsorption and desorption of U(VI) on functionalized graphene oxides: a combined experimental and theoretical study. Environ Sci Technol 49:4255–4262
47. Sun YB, Wang Q, Chen CL, Tan XL, Wang XK (2012) Interaction between Eu(III) and graphene oxide nanosheets investigated by batch and extended X-ray absorption fine structure spectroscopy and by modeling techniques. Environ Sci Technol 46:6020–6027
48. Ren X, Wang S, Yang S (2010) Influence of contact time, pH, soil humic/fulvic acids, ionic strength and temperature on sorption of U(VI) onto MX-80 bentonite. J Radioanal Nucl Chem 283:253–259
49. Montavon G, Markai S, Andres Y, Grambow B (2002) Complexation studies of Eu(III) with alumina-bound polymaleic acid: effect of organic polymer loading and metal ion concentration. Environ Sci Technol 36:3303–3309
50. Sun YB, Shao DD, Chen CL, Yang SB, Wang XK (2013) Highly efficient enrichment of radionuclides on graphene oxide-supported polyaniline. Environ Sci Technol 47:9904–9910
51. Sun YB, Li JX, Wang XK (2014) The retention of uranium and europium onto sepiolite investigated by macroscopic, spectroscopic and modeling techniques. Geochim Cosmochim Acta 140:621–643
52. Pourbeyram S (2016) Effective removal of heavy metals from aqueous solutions by graphene oxide-zirconium phosphate (GO-Zr-P) Nanocomposite. Ind Eng Chem Res 55:5608–5617
53. Sheng G, Shao D, Fan Q, Xu D, Chen Y, Wang X (2009) Effect of pH and ionic strength on sorption of Eu(III) to MX-80 bentonite: batch and XAFS study. Radiochim Acta 97:621–630
54. Langmuir I (1918) The adsorption of gases on plane surfaces of glass, mica and platinum. J Am Chem Soc 40:1361–1403
55. Kilpatrick M, Baker LL (1955) A study of fast reactions in fuel-oxidant system: anhydrous hydrazine with 100 per cent nitric acid. Symp (Int) Combust 5:196–205
56. Rajapaksha AU, Vithanage M, Ahmad M (2015) Enhanced sulfamethazine removal by steam-activated invasive plant-derived biochar. J Hazard Mater 290:43–50
57. Shahwan T, Erten HN (2004) Temperature effects in barium sorption on natural kaolinite and chlorite-illite clays. J Radioanal Nucl Chem 260:43–48

58. Yang ST, Sheng GD, Tan XL, Hu J, Du JZ, Montavon G, Wang XK (2011) Determination of Ni(II) uptake mechanisms on mordenite surfaces: a combined macroscopic and microscopic approach. Geochim Cosmochim Acta 75:6520–6534
59. Li J, Zhang S, Chen C, Zhao G, Yang X, Li J, Wang X (2012) Removal of Cu(II) and fulvic acid by graphene oxide nanosheets decorated with Fe_3O_4 nanoparticles. ACS Appl Mater Inter 4:4991–5000
60. Chen C, Wang X (2006) Adsorption of Ni(II) from aqueous solution using oxidized multiwall carbon nanotubes. Ind Eng Chem Res 45:9144–9149
61. Badruddoza AZM, Tay ASH, Tan PY, Hidajat K, Uddin MS (2011) Carboxymethyl-b-cyclodextrin conjugated magnetic nanoparticles as nano-adsorbents for removal of copper ions: synthesis and adsorption studies. J Hazard Mater 185:1177–1186
62. Fan Q, Shao D, Lu Y, Wang S, Wang X (2009) Effect of pH, ionic strength, temperature and humic substances on the sorption of Ni(II) to Na-attapulgite. Chem Eng J 150:188–195
63. Fan Q, Tan X, Li J, Wang X, Wu W, Montavon G (2009) Sorption of Eu(III) on attapulgite studied by batch, XPS, and EXAFS techniques. Environ Sci Technol 43:5776–5782
64. Zhao G, Ren X, Gao X, Tan X, Li J, Chen C, Huang Y, Wang X (2011) Removal of Pb(II) ions from aqueous solutions on few layered graphene oxide nanosheets. Dalton Trans 40:10945–10952